UCRL - 75094
PREPRINT
CONF-730958--1

LAWRENCE LIVERMORE LABORATORY
University of California/Livermore, California

Excitation States of Projectiles Moving Through Solids

R. J. Fortner

and

J. D. Garcia

September 1973

This Paper was Prepared For Presentation at

The Third International Conference on Atomic Collisions in Solids
Gatlinburg, Tenn. 9/23-28/73

Excitation States of Projectiles Moving Through Solids*

R. J. Fortner
Lawrence Livermore Laboratory, Livermore, CA 94550

J. D. Garcia†
University of Arizona, Tucson, Arizona 85721

Abstract

X-ray spectral measurements of S, Cl, and Ar atoms moving in solid carbon targets are used to extract the equilibrium distribution of vacancies in the valence and L-shells of the projectiles. It is found that the state of excitation is much higher than the mean charge measured after the projectile has left the solid. A simple model is used to deduce the expected final charge state distribution, and these are compared to thin foil measurements. Our results support the Betz-Grodzins model for ions moving in solids.

*Work performed under the auspices of the U. S. Atomic Energy Commission.
†Supported in part by grants from the NASA, ONR, and NSF.

In this paper x-ray spectral measurements of projectiles traversing a solid are used to determine equilibrium distribution of vacancies in the inner and valence shells of the projectile. Disparity between our measurements and the measured emergent charge states is used to support the Betz-Grodzins model[1] for ions moving in solids. A simple picture based on the Betz-Grodzins model is found to bring the two measurements into agreement.

The relevant data used in this paper are presented in Figs. 1 and 2. Figure 1 shows the spectral data[2,3] for S, Cl, Ar → C collisions using a solid graphite target and an incident projectile energy of 90 keV. The arrows in the figure indicate the positions of the normal (unshifted) x-ray transitions. The data indicate that the majority of the x-rays are L x-rays from the projectile; however, some carbon K x-rays are observed. Identification of the x-ray transitions is discussed below. Figure 2 shows the x-ray production cross sections for both target and projectile in the Ar → C collision system as determined from the x-ray spectral measurements.[4]

Multiple L-shell vacancies can be produced in the projectile due multiple collisions in the solid within the lifetime of an inner shell hole. The lifetime of a ground state sulphur L-shell vacancy is 5×10^{-14} sec.[5] This can be compared with the mean free time for producing an L-shell vacancy, $1/N\sigma v$, where N is the number of carbon atoms per cm^3, σ is the L-shell vacancy production cross section (in cm^2) and v is the velocity of the projectile in cm/sec. The cross section can be estimated[6] to be $\sim 10^{-17}$ cm^2. This leads to a mean free time for producing an L-shell vacancy in 90 keV S^+ - C collisions of about 10^{-14} sec.

Thus, each ion having an L-shell vacancy undergoes several collisions of this type during the lifetime of the vacancy. L-shell vacancies are not expected to be produced in the projectile when the 2p binding energy of projectile exceeds the 1s binding energy of carbon. This is due to changes in the molecular orbital diagrams[7] which are normally used to described these collisions. The changes result in the inner shell vacancies being produced in the carbon K shell rather than the projectile. This results in a limitation in the number of L-shell vacancies of 4, 2, and 1 for S, Cl, and Ar, respectively.[8]

The general theoretical formulation of this problem is straightforward. Let f_i be the fractional probability of beam having i inner shell vacancies and let q be the maximum number of vacancies determined by the discussion above. Assuming thin targets and neglecting double electron processes, the production and decay of inner shell vacancies in any thickness dx of the solid is determined by the following equations.

$$f_0 + f_1 + \cdots + f_q = 1 \qquad (1)$$

$$\frac{df_0}{dx} = f_1/v\tau_1 - N\sigma_0 f_0$$

$$\frac{df_1}{dx} = N\sigma_0 f_0 - f_1/v\tau_1 + f_2/v\tau_2 - N\sigma_1 f_1$$

$$\cdots\cdots$$

$$\frac{df_{q-1}}{dx} = N\sigma_{q-2} f_{q-2} - f_{q-1}/v\tau_{q-1} + f_q/v\tau_q - N\sigma_{q-1} f_{q-1}$$

$$\frac{df_q}{dx} = N\sigma_{q-1} f_{q-1} - f_q/v\tau_q$$

where N is number of target atoms per cubic centimeter, v is the velocity of the projectile, τ_i is the lifetime of the projectile having i inner shell vacancies and σ_i is the cross section for i to $i + 1$ inner shell vacancies. For $q = 1$ the solution of Eq. (1) yield

$$f_1 = \frac{N\sigma_0 v\tau_1}{1+N\sigma_0 v\tau_1} \left(1 - \exp - \left[\left(N\sigma_0 + \frac{1}{v\tau_1}\right) x\right]\right). \qquad (2)$$

For $q > 1$ solutions of Eq. (1) can be obtained but, the more relevant quantities, the equilibrium fractions can be determined simply by setting the derivaties equal to zero. When this is done Eq. (1) yields

$$f_i = \prod_{j=1}^{i} (N\sigma_{j-1} v\tau_j) \Big/ \left[1 + \sum_{k=1}^{q} \prod_{j=1}^{k} (N\sigma_{j-1} v\tau_j)\right] \qquad (3)$$

or

$$f_i = N\sigma_{i-1} v\tau_i f_{i-1}$$

Equations (2) and (3) can be used to estimate equilibrium fractions of projectile inner shell vacancies. Before this is done we must determine the total ionization cross section and the inner shell lifetimes for the appropriate states. Therefore, we must consider the effects of M-shell vacancies using the observed x-ray spectra in Fig. 1.

The L x-ray energy shifts observed can be understood from the following: the projectile moving in the graphite target suffers a small-impact-parameter collision which produces the L-shell vacancy, considerable M-shell excitation might also be expected. However, as the projectile with the inner shell vacancy continues to move in the solid, other larger-impact-parameter collisions will change the state

of the M-shell by a variety of processes (e.g., charge exchange, electron pick-up etc.). Using a nominal cross section of 10^{-16} cm^2 for these processes[1] the mean free time for such events is 10^{-15} sec. Thus, on the average, 50 such events will take place for the sulphur projectile before the inner shell vacancy is filled. We conclude that the M-shell of the moving ion will return to an equilibrium distribution prior to the filling of the L-shell vacancy. Thus, the observed shifts in the projectile x-ray spectra are characteristic of an equilibrium distribution of M-shell vacancies. Note that the particular transitions observed are only weakly affected by electrons in N or higher shells.

In Table I the results of Hartree Fock (adiabatic) calculations[8] of the energy shift of the 3s → 2p L x-ray transition as a function of M-shell excitation are presented. Also included in the table are theoretical values of the fluorescence yields[9,10] for each configuration. The chlorine values for energy shifts and fluorescence yield were obtained by extrapolation between the values for sulphur[8,10] and argon.[9-11] The direct calculations of sulphur fluorescence yields were compared with those obtained via statistical corrections[11-12] to ground state fluorescence yields and only small differences were found (less than 30%). Additional calculations were done to determine the effects of multiple inner shell vacancies on x-ray transition energies for the case of sulphur. The results indicated that a positive shift of ~25 eV occurs for each additional 2p vacancy. Calculations also indicated that for sulphur, the position of a 3d → 2p transition is ~25 eV higher than a 3s → 2p transition with the same initial configuration.

Using the above calculations the analysis of spectra in Fig. 1 is straightforward. In the S^{6} - C data, for example, the peak in the spectrum (at 168 eV) corresponds to a 3s → 2p transition in a sulphur atom with one 2p vacancy and only one 3s electron in the M-shell. This peak is enhanced in the spectrum because of a large fluorescence yield (1.0). The other x-rays between 147 eV and 168 eV represent the same transition but with differing numbers of M-shell electrons. The L x-rays above 168 eV are due to multiple L-shell vacancies (and possibly some 3d → 2p transitions). In fact, in the sulphur data, x-rays corresponding to atoms with as many as 4 L-shell vacancies are observed. The photons at 277 eV are carbon K x-rays; the mechanisms responsible for production of these x-rays was discussed above. Similar observations can be made for the Cl, Ar - C data. In the chlorine and argon case, x-rays due to 2 and 1 L-shell vacancies, respectively, can be seen.

The relative probability of the projectile having a given number of M-shell vacancies can be calculated from the x-ray spectra using the data in Table 1. Some assumption must be made concerning the relative probabilities of 3s and 3p vacancies (our calculations indicate that Coster-Kronig transitions in the M-shell are energetically not allowed in an atom with an L-shell vacancy). In our analysis we assumed sequential stripping, but the assumption was tested as indicated below. The x-ray spectra are characteristic of thick targets and thus standard thick target yield analysis is required; however, this made little difference in the results.

In Fig. 3 the results of our analysis are presented. In the analysis of these spectra corrections for window absorption[13] and crystal reflectivity[14] were made. Assumptions other than sequential stripping (such as statistical

distribution of the M-shell vacancies among the M-subshells) resulted in enhancement of the higher states of M-shell excitation. Thus, the sequential stripping assumption results in a lower bound determination of the mean number of M-shell vacancies, which is larger than the mean emergent charge state (see below).

Using the results presented in Fig. 3, we can determine the mean value of fluorescence yield and the mean life time for the inner shell vacancy. This, in conjunction with Fig. 2 and Eq. 2, can be used to determine equilibrium fraction of argon ions with an inner shell vacancy. The results of this analysis are presented in Table 2. We have included in the table the parameter $r = N_0 \sigma v \tau_1 = \lambda_{decay}/\lambda_{production}$ where the λ's are the appropriate mean free paths for the inner shell vacancies. In Table 3, the relative fraction of L shell vacancies for a 90-keV sulphur projectile determined from Eq. 3, using a cross section $\sigma_i = \frac{6-i}{6}\sigma_0$ where σ_0 was estimated to be 10^{-17} cm^2. We also asssumed the lifetime for multiple L-shell holes was the same as that for a single L-shell hole. As can be seen from the table, large numbers of L-shell vacancies are expected.

Measurements of the charge state populations of Ar emerging from carbon foils are available.[15] In order to compare our results for projectiles within the solid with these results, some statement concerning the state of the projectile as it leaves the solid must be made. Using our equilibrium distribution for L- and M-shell vacancies in the projectile, we assume that (1) the missing M-shell electrons are carried with the ion in higher shells; (2) when the ion emerges from the solid it loses (a) one electron for each inner shell vacancy due to Auger processes, and (b) one electron for each electron pair

in shells higher than the M-shell due to autoionizing processes. The resultant distribution labelled BG is shown in Fig. 4 together with the (interpolated) data of Hvelplund et al.[15]

These results indicate that analysis of x-ray spectra can be used as a practical tool for investigating equilibrium excitation states of ions traversing a solid. They also provide strong support for the model introduced by Betz and Grodzins (BG) (see Ref. 1, p. 533) in connection with the density effect. They proposed that ions moving in solids are essentially neutral but in a high state of excitation. This is in contrast with the Bohr-Lindhard model (BL), in which the ion moves through the solid essentially with its emergent mean charge state, and at most, one-electron excitation. In the present work, if the projectiles emerged without accompanying electrons and with the L- and M-shell vacancy distributions as observed, the emergent mean charge states would be the distribution labelled BL in Fig. 4. This predicts higher charge states than those actually observed. It should be kept in mind that the electrons accompanying the ion in shells higher than the M-shell will have negligible effects on the x-ray energies or rates. The fact that simple assumptions, which are in agreement with the BG model, can correlate the final charge state measurements and our reported vacancy distributions provides the first direct experimental evidence concerning the validity of either model.

TABLE I - Theoretical data for multiply ionized S, Cl, and Ar for transitions from the configuration $1s^2\ 2s^2\ 2p^5\ 3s^n\ 3p^m$.

		X-Ray Energy Shift (eV)[a]			Fluorescence Yield x 10^4		
n	m	Sulphur	Chlorine	Argon	Sulphur	Chlorine	Argon
2	6	-	-	N[b]	-	-	1.9
2	5	-	N[b]	2.9	-	1.9	2.7
2	4	N[b]	2.9	7.0	1.9	2.8	4.1
2	3	3.0	7.1	11.8	2.9	4.7	6.9
2	2	7.2	12.0	17.4	5.5	8.8	14.0
2	1	12.1	17.5	23.7	15.6	25.5	40.0
2	0	17.7	24.0	30.8	77.4	105.0	15%.
1	6	-	-	-	-	-	1.1
1	5	-	-	-	-	1.05	1.6
1	4	-	-	-	1.0	1.65	2.5
1	3	-	-	-	1.7	2.8	4.3
1	2	11.2	-	-	3.9	6.6	10.9
1	1	15.4	-	-	18.2	32.0	53.9
1	0	21.1	29.2	36.0	10^4	10^4	10^4

a) Hartree-Fock adiabatic calculations (Ref.8). The energy shifts depend primarily on n + m. In that part of the table for n = 1, only significant deviations from this rule are noted.

b) Ground state value; this is the reference point for the shifts.

TABLE 2: Data on equilibrium distribition of L-shell vacancies in an argon beam traversing a solid carbon target.

E (keV)	r	f_1(Ar)	$(N\sigma_o+1/v\tau_1)^{-1}$
30	.20	.17	73 Å
45	.39	.28	75 Å
60	.58	.37	78 Å
90	.88	.47	80 Å
130	1.24	.55	81 Å
180	1.60	.62	82 Å

TABLE 3: Estimated data on equilibrium distribution of L-shell vacancies in a 90-keV sulphur beam traversing a solid carbon target.

f_0 - .086

f_1 - .156

f_2 - .232

f_3 - .276

f_4 - .250

References

1. H. D. Betz, Rev. of Mod. Phys. 44, 465 (1972).
2. R. C. Der, R. J. Fortner, T. M. Kavanagh, J. D. Garcia, Phys. Rev. Letters 27, 1631 (1971).
3. R. J. Fortner, R. C. Der, T. M. Kavanagh, and J. D. Garcia (to be published).
4. R. J. Fortner, R. C. Der, and J. D. Garcia (to be published).
5. D. L. Walters and C. P. Bhalla, Phys. Rev. A4, 2164 (1971).
6. F. W. Saris and D. Onderdelinden, Physica 49, 441 (1970).
7. M. Barat and W. Lichten, Phys. Rev. A6, 211 (1972).
8. J. D. Garcia, R. J. Fortner, and J. Schofield (to be published).
9. F. P. Larkins, J. Phys. B4, L29 1971).
10. C. Bhalla, this conference.
11. F. P. Larkins, J. Phys. B4, 14 (1971).
12. R. J. Fortner, R. C. Der, T. M. Kavanagh, and J. D. Garcia, J. Phys. B5, L73 (1972).
13. M. A. Spivack, Rev. Sci. Instr. 41, 1614 (1970).
14. B. L. Henke, Advances in X-ray Analysis 7, 460 (1963).
15. P. Hvelplund, E. Laegsgard, J. O. Olsen, and E. H. Pedersen, Nuc. Instr. & Methods 90, 315 (1970).

Fig. 1. X-ray spectra for Ar + C (upper diagram) Cl + C (middle diagram), and S + C (lower diagram) collisions in solid (graphite) targets. The positions of the "normal" (unshifted) L x-rays are indicated by labelled arrows as is the position of the C K x-ray line. The bombarding energy was 90 keV. In the lower diagram, the carbon K x-rays produce a second order peak at about 140 keV. The dashed line shows the resultant spectrum when the second order carbon line is subtracted, by using the first order profile.

Fig. 2. X-ray production cross sections for Ar_L and C_K resulting from Ar + C collisions in solid (graphite) targets.

Fig. 3. Equilibrium M-shell vacancy distribution for 90 keV S (diamonds), Cl (open circles) and Ar (triangles) ions traversing a carbon solid target.

Fig. 4. Charge state distributions for 90 keV Ar projectiles emerging from a carbon foil. Diamonds denote the measurements of Hvelplund et al.; circles and squares are the results of the present analysis (see text).

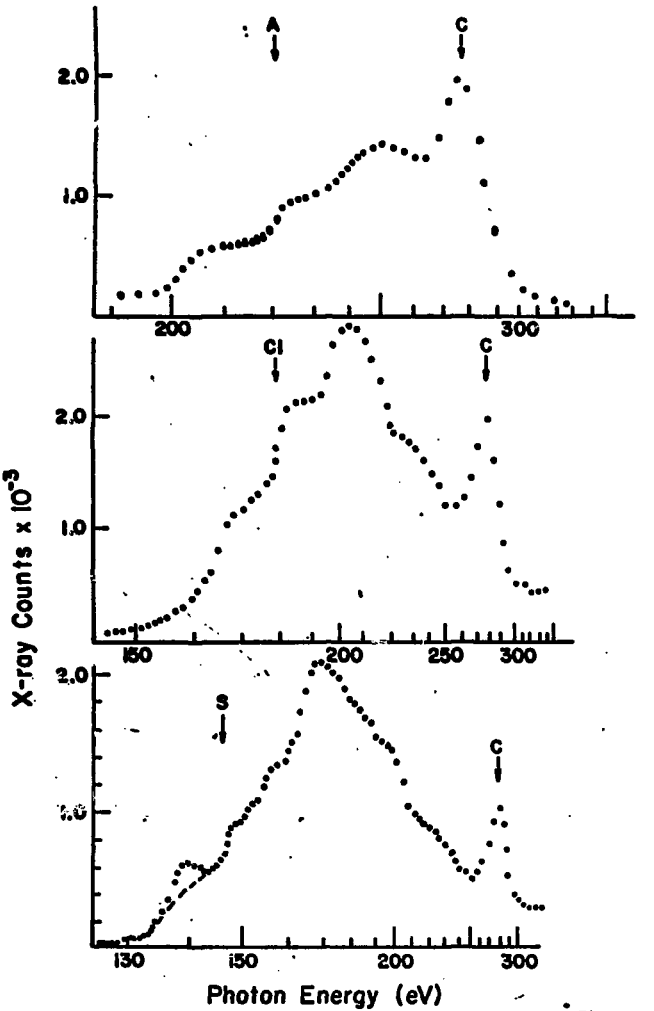
A
C
2.0
1.0
200
300
Cl
C
2.0
1.0
150
200
250
300
S
C
2.0
1.0
130
150
200
300
X-ray Counts x 10⁻³
Photon Energy (eV)

Fig. 1

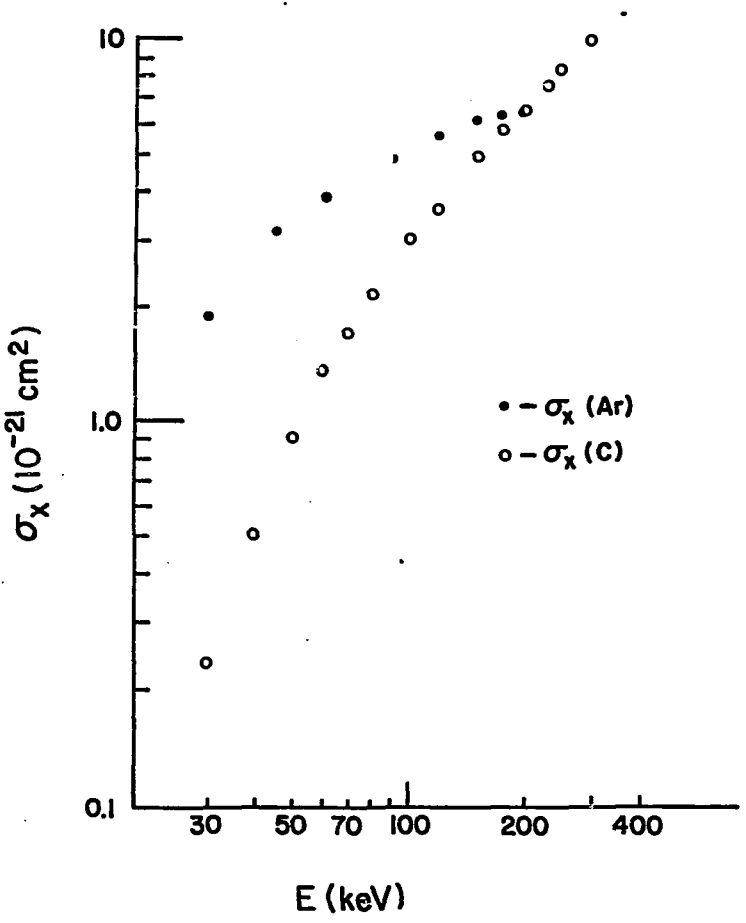
10
1.0
0.1
σ_x (10^{-21} cm^2)
• – σ_x (Ar)
o – σ_x (C)
30
50
70
100
200
400
E (keV)

Fig. 2

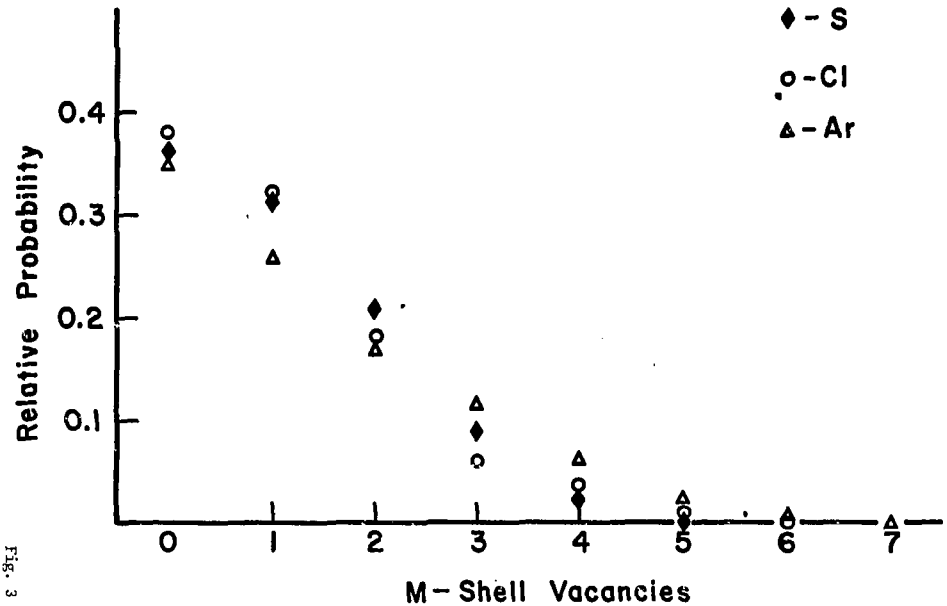
♦ - S
o - Cl
△ - Ar
Relative Probability
0.4
0.3
0.2
0.1
0
1
2
3
4
5
6
7
M - Shell Vacancies

Fig. 3

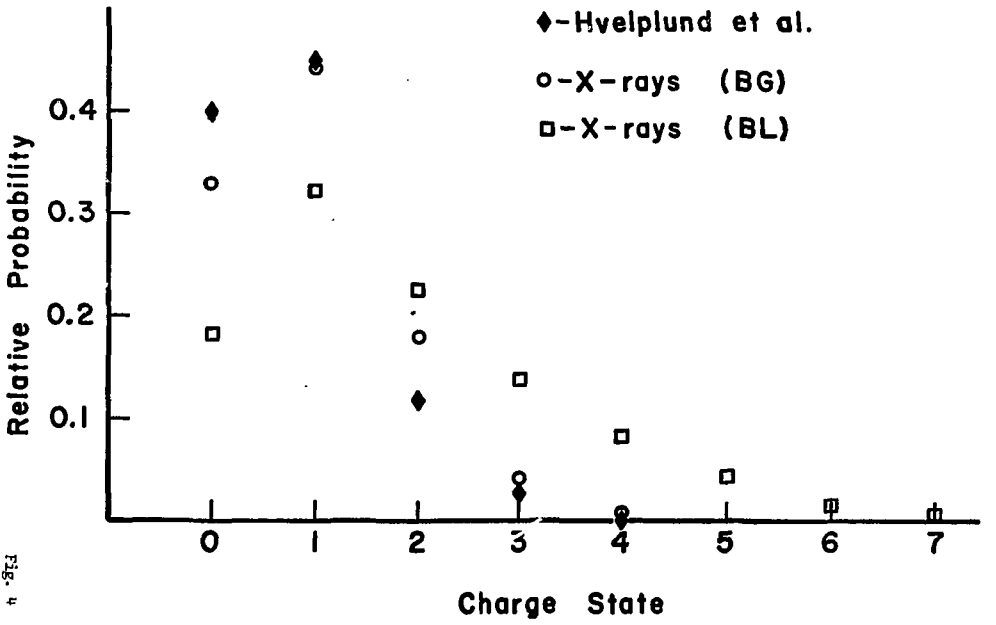
♦-Hvelplund et al.
o-X-rays (BG)
□-X-rays (BL)
Relative Probability
0.4
0.3
0.2
0.1
0
1
2
3
4
5
6
7
Charge State